Enzyme Nanotechnology

Deutsche Ausgabe: DOI: 10.1002/ange.201500981
Internationale Ausgabe: DOI: 10.1002/anie.201500981

Cross-β Amyloid Nanohybrids Loaded With Cytochrome C Exhibit Superactivity in Organic Solvents**

*Nidhi Kapil, Ashmeet Singh, and Dibyendu Das**

Abstract: *The present study reports the development of a unique class of Cytochrome C (CytC)-loaded cross-beta amyloid nanohybrids. The peroxidase activity of the bound CytC increased up to two orders of magnitude in organic solvents compared to the activity of unbound CytC in water. The amyloid sequences used in the study feature the nucleating core ^{17}LVFF^{21} of the beta amyloid (Aβ), which assembled to form homogenous fibers and nanotubes. The morphology and exposed surface of the amyloid nanohydrids critically modulated the CytC activity. A CytC–Ac-KLVFFAE-NH_2 hybrid featuring nanofiber morphology showed 308-fold higher activity than unbound CytC in water, which increased to 450-fold with the nanotube morphology of CytC–Ac-KLVFFA**L**-NH_2. Notably, activity declined substantially when the exposed surface charge was detuned by replacing lysine with histidine, thus underpinning the importance of surface charge. This enzyme–amyloid nanohybrid system could facilitate the technological application of enzymes.*

Deposits of cross-β protein fibers (named for the cross-shaped pattern they produce under X-ray diffraction) accumulate in many neurodegenerative diseases, with Alzheimer's disease (AD) being one of the most studied.[1] AD is associated with the formation of these plaques in the brain, and homogenous fibrillar tangles are observed when imaged under a microscope.[1] The self-assembled robust nanostructures are held together by weak noncovalent forces and in-depth studies have provided insight into their modes of interaction.[1b,2] The wildtype beta amyloid Aβ(1–42) has been explored in detail and its various segments have been probed for their self-assembly efficacies.[1b] These studies have resulted in the discovery of specific nicks in the amphiphilic sequence that can act as nucleating cores, and this knowledge has substantially helped in deciphering the rules of self-assembly governing the formation of these stacks of β sheets inside living systems.[1b,2a,d] These investigations have also contributed to the design of novel amyloid-based functional materials.[3] Reports have shown that the introduction of mutations through rational design can create remarkably homogenous nanostructured materials with advanced functions.[3a,b,4] Another exciting facet of these soluble structures is their capability to noncovalently bind molecules of diverse nature and dimensions, from small molecules such as Congo Red and Thioflavin T to macromolecules such as proteins and nucleic acid oligomers.[1b,5] For instance, small peptide amphiphiles were explored to immobilize and activate proteins in organic solvents in some elegant studies by Xu and coworkers[4k–n]. They further observed that proteins have excellent stability when immobilized in molecular gels of peptide nanostructures.[4k–n] The capability of amyloid nanostructures to bind diverse molecular architectures in a precise order arises from the multitude of interaction sites displayed on their surfaces. The diagnostic apple-green birefringence observed upon the addition of Congo Red is due to specific molecular alignment onto these amphiphilic nanosurfaces, which offer hydrophobic and ionic interactions.[5a]

We envisaged that the propensity of amyloid nanostructures to noncovalently bind proteins and small molecules, combined with the amphiphilicity of these soluble nanophases, could increase enzyme activity under non-aqueous conditions by augmenting the mass transport of substrates/products (Figure 1 A). In the present study, a unique class of CytC-loaded amyloid nanohybrids (Figure 1) was discovered, for which the activity of the CytC peroxidase was improved by two orders of magnitude in organic solvents compared to the activity of unbound enzyme in water. The β-amyloid sequences containing ^{17}LVFF^{21} nucleating core were judiciously altered to understand the role of exposed surface and morphology on the superactivity of CytC.

The soluble amyloid nanostructures were initially added exogenously during CytC activity measurements. We started with the self-assembling motif of Ac-KLVFFAE-NH_2 (Figure 1 B), from residues 16–22 of wildtype Aβ. Ac-KLVFFAE-NH_2 exhibited characteristic antiparallel β-sheet secondary structure signatures (Figure S1 in the Supporting Information). Amyloid nanofibers of approximately 15 nm diameter with lengths reaching several micrometers (Figure 1 C) could be observed by transmission electron microscopy (TEM). For enzyme activity measurements, 15 μL of free CytC (83.3 mg mL^{-1} in water) was added to a round-bottomed flask followed by 7.7 μL of a 2.5 mM stock of Ac-KLVFFAE-NH_2 (see the Supporting Information). After approximately 30 min incubation, toluene (25 mL) was added followed by addition of the substrate pyrogallol (final concentration 10 mM) and different concentrations of H_2O_2. This model reaction was chosen because of hydrophilic nature of pyrogallol (log *P* 0.294) and the hydrophobic product purpurogallin (log *P* 2.416) which has similar hydrophobicity to the

[*] N. Kapil, A. Singh, Dr. D. Das
Institute of Nano Science and Technology
Phase 10, Mohali 160062 (India)
E-mail: ddas@inst.ac.in
ddas.chem@gmail.com

[**] D.D. and N.K. are thankful to DST, India financial assistance through INSPIRE Faculty Grant (No. IFA12-CH-64). A.S. acknowledges UGC, India for a Fellowship. D.D. acknowledges Dr. M. Singh, Dr. S. Vaidyafor EM imaging and Dr. K. Hazra for AFM imaging.

Supporting information for this article is available on the WWW under http://dx.doi.org/10.1002/anie.201500981.

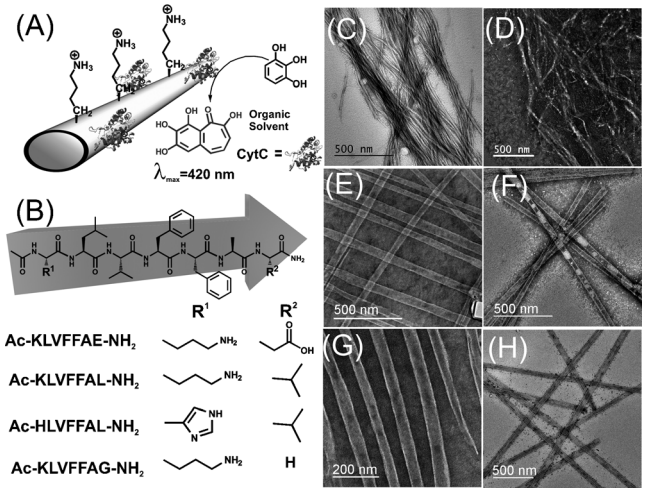

Figure 1. A) Schematic representation of the activity of CytC–amyloid nanohybrids in organic solvent. B) Structures of the amyloid peptides. C–H) TEM micrographs of self-assembled nanofibers of Ac-KLVFFAE-NH_2 without CytC (C) and with CytC (D), nanotubes of Ac-KLVFFA**L**-NH_2 without CytC (E) and with CytC (F), and nanotubes of Ac-**H**LVFFA**L**-NH_2 without CytC (G) and with CytC (H).

solvent toluene ($\log P$ 2.678). This should enhance the catalytic process by facilitating diffusion.[4l,m,6] The progress of the reaction was monitored from the formation of purpurogallin and the bimolecular rate equation depends on the concentration of CytC and H_2O_2 (see Equation S1 and Figure S2 in the Supporting Information).[6] Interestingly, in presence of Ac-KLVFFAE-NH_2, the activity of CytC showed a nine-fold improvement compared to free CytC in water (0.11 $\mu M\,s^{-1}\,\mu g^{-1}$ for 60 mM H_2O_2; under the same experimental conditions, the activity of free CytC in water was 0.0126 $\mu M\,s^{-1}\,\mu g^{-1}$). To investigate the role of morphology, the glutamic acid residue in Ac-KLVFFAE-NH_2 was mutated to a leucine residue to form Ac-KLVFFA**L**-NH_2,[5a] which assembles into homogenous nanotubes of diameter $d = 35 \pm 8.0$ nm (Figure 1E). In the presence of Ac-KLVFFA**L**-NH_2 nanotubes, the activity of CytC was 0.143 $\mu M\,s^{-1}\,\mu g^{-1}$, which is 12-fold higher than its activity in water (Figure S3). Although minor, this activation is significant since no measurable activity was observed over more than 2 h in control experiments with unbound CytC in toluene without amyloid nanostructures, thus underpinning the importance of the amyloid in the possible augmentation of mass transport.

At this point, we thought that instead of using amyloid nanostructures as additives, it would be intriguing to investigate their activating role when CytC is exclusively loaded onto their surfaces. To obtain CytC-loaded amyloid nanohybrids, CytC (40 $mg\,mL^{-1}$) and amyloid nanostructures (2.5 mM) were mixed in aqueous solution and incubated for 30 min and then centrifuged, which produced a red pellet. To remove unbound protein, the pellet was washed twice through a process of redispersion and centrifugation and the nanohybrids were found to retain their morphology (Figure 1). Interestingly, brighter regions were observed throughout the nanofibers of Ac-KLVFFAE-NH_2 (Figure 1D). In the case of Ac-KLVFFA**L**-NH_2 nanotubes, unstained globular bright regions could be observed on the surface (Figure 1F), thus indicating the formation of CytC-bound amyloid nanohybrids. To estimate protein loading, the supernatant was subjected to Bradford Assay (see the Supporting Information). For Ac-KLVFFAE-NH_2 fibers and Ac-KLVFFA**L**-NH_2 tubes, 478 ± 21 μg and 512 ± 25 μg of CytC was found to be loaded, respectively (Table S1 and Figure S4).

Strikingly, CytC–Ac-KLVFFAE-NH_2 nanohybrids showed CytC activity of 3.69 $\mu M\,s^{-1}\,\mu g^{-1}$, which is 308-fold higher than the activity shown by unbound CytC in water (Figure 2 and Table S2). The activity of CytC in the nanohybrids containing Ac-KLVFFA**L**-NH_2 nanotubes further increased to 5.4 $\mu M\,s^{-1}\,\mu g^{-1}$, which is up to 450-fold higher than that for unbound CytC (Figure 2, Figure S5, and Table S3 for activity in different solvents).[6]

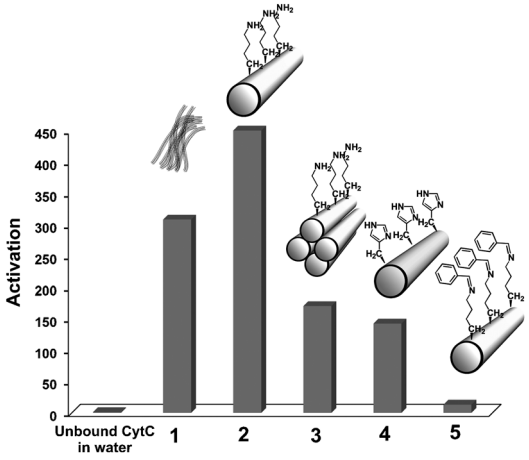

Figure 2. Activation in toluene (relative to that of unbound CytC in water) of CytC bound to Ac-KLVFFAE-NH_2 nanofibers (1), Ac-KLVFFA**L**-NH_2 nanotubes (2), bundled Ac-KLVFFA**L**-NH_2 nanotubes treated with Na_2SO_4 (3), Ac-**H**LVFFA**L**-NH_2 nanotubes (4), and Ac-KLVFFA**L**-NH_2 nanotubes with benzaldehyde treatment (5). [Pyrogallol = 10 mM]; [H_2O_2] = 60 mM. Experimental errors were within ±5–15%.

To investigate this remarkable activation seen with the Ac-KLVFFA**L**-NH_2 nanotubes, the nanohybrids were further characterized by atomic force microscopy (AFM; Figure 3). Without CytC, nanotubes of approximately 10–11 nm in height could be seen, while in presence of CytC, distinct globular structures were observed on the surface of nanotubes (Figure 3A,B). Line analysis showed that in sections containing the globular structures, the height increased from 10.9 nm to 17.6 nm (Figure 3C). However, some irregular structures were also observed in nanotubes without CytC (Figure 3A). Hence, to confirm that CytC is indeed loaded onto the nanotubes, the protein was tagged with a fluorophore. CytC was covalently conjugated to fluorescein isothiocyanate (FITC) and purified over a Sephadex G-25M column. CytC–FITC–Ac-KLVFFA**L**-NH_2 was prepared by following a similar protocol to that used previously (see the Supporting Information) and the hybrids retained the nanotube morphology (Figure 4A). Fluorescent tubular structures were observed when these nanohybrids were imaged by

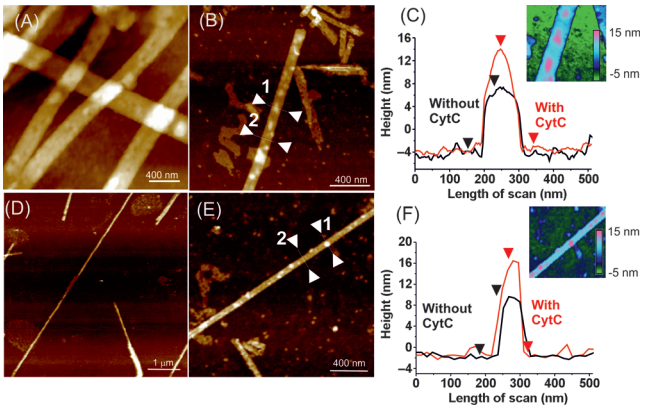

Figure 3. A–C) Ac-KLVFFA**L**-NH_2: AFM images are shown for the self-assembled nanotubes without (A) and with (B) CytC, and a line scan reveals the heights of the tubes with and without CytC (C). D–F) Ac-**H**LVFFA**L**-NH_2: AFM images are shown for the self-assembled nanotubes without (D) and with (E) CytC, and a line scan reveals the heights of the tubes with and without CytC (F). Insets show AFM images color-coded for height.

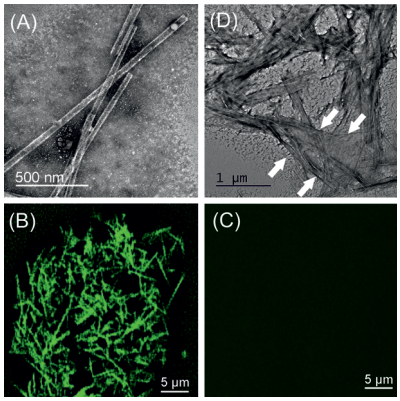

Figure 4. A) TEM image of Ac-KLVFFA**L**-NH_2 loaded with CytC–FITC. B, C) Fluorescence microscopy images (excited at 495 nm) of Ac-KLVFFA**L**-NH_2 nanotubes loaded with CytC–FITC (B) and Ac-KLVFFA**L**-NH_2 alone (C). D) TEM image of CytC-Ac-KLVFFA**L**-NH_2 nanohybrids bundled with Na_2SO_4, with arrows indicating bundles of nanotubes.

fluorescence microscopy (Figure 4B). No such structures were observed in the control tubes without CytC–FITC (Figure 4C). The fluorescence microscopy results thus confirmed the formation of protein-loaded amyloid nanohybrids.

The remarkably increased CytC activity observed in the nanohybrids could be due to enhanced mass transfer facilitated by the amyloid nanostructures.[6a,7] In this context, substrate/product transport would critically depend on the solvent-exposed surface of dispersed amyloid nanohybrids, particularly the surface area and the exposed charge. To confirm the importance of surface area of dispersed nanotubes, Na_2SO_4 was added to protein amyloid nanohybrids to bundle the nanotubes.[8] Indeed, TEM showed bundles of CytC–Ac-KLVFFA**L**-NH_2 nanohybrids (Figure 4D). The activity of CytC in the bundled nanohybrids decreased from 5.4 $\mu M\,s^{-1}\,\mu g^{-1}$ to 1.68 $\mu M\,s^{-1}\,\mu g^{-1}$ (Figure 2). The lower activity in bundled tubes illustrates the importance of exposed surface. Based on a similar argument, the higher activation effects observed in case of Ac-KLVFFA**L**-NH_2 nanotubes in comparison to Ac-KLVFFAE-NH_2 fibers could be attributed to the higher charge density of the nanotubes. The sequence Ac-KLVFFAE-NH_2 self-assembles in antiparallel in-register[2a] cross-β fibers (Figure S1A,B), which results in the exposure of two kinds of solvent-facing surfaces over four facets. Out of these four facets, two have charged surfaces made from saturated salt bridges between lysine and glutamic acid residues, while the other two facets have side chains exposed to the solvents.[2a] In Ac-KLVFFA**L**-NH_2 on the other hand, the mutation of glutamic acid to leucine means that the formed nanotubes have out-of-register bilayer structures with cationic lysine residues coating the inner and outer surfaces.[5a] This enhanced cationic charge density in Ac-KLVFFA**L**-NH_2 might facilitate the exit of hydrophobic Purpurogallin. To further support this argument, the cationic charge of Ac-KLVFFA**L**-NH_2 was detuned through mutation of the lysine residue to the less basic histidine, which has a substantially lower hydropathy index (−3.2 for histidine vs −3.9 for lysine).[9] Ac-**H**LVFFA**L**-NH_2 forms cross-β nanotubes (Figure 1G, Figure 3D, and Figure S1) and the CytC hybrids were characterized by TEM and AFM (Figure 1H, Figure 3E,F). The decreased charge was indeed important since CytC–Ac-**H**LVFFA**L**-NH_2 hybrids showed substantially lower activity (2.04 $\mu M\,s^{-1}\,\mu g^{-1}$) than CytC–Ac-KLVFFA**L**-NH_2; however the activity was still 170-fold higher than that for unbound CytC in water (Figure 2). To support the significance of free lysine residues on activation, benzaldehyde was added to condense the free lysine residues to their corresponding Schiff bases, which would result in reduction of the surface charge (see the Supporting Information). The activity of benzaldehyde-functionalized Ac-KLVFFA**L**-NH_2 nanohybrids plummeted to 0.14 $\mu M\,s^{-1}\,\mu g^{-1}$, a mere 2.6% of the activity shown in absence of benzaldehyde. Benzaldehyde had no effect on the activity of unbound CytC. These results underpin the importance of charged lysine on amyloid nanosurface for CytC activation. The role of C-terminal hydrophobicity was investigated through mutation of the leucine to a glycine residue to form Ac-KLVFFA**G**-NH_2, which also forms nanotubes (Figure S6). The activity of CytC–Ac-KLVFFA**G**-NH_2 was found to be 4.6 $\mu M\,s^{-1}\,\mu g^{-1}$, which is approximately 85% of the activity observed with Ac-KLVFFA**L**-NH_2 (Table S2). Although the activity is slightly lower, the change is not as drastic as the change with mutation of the N-terminal lysine to a histidine residue. Apart from facilitated mass transport, the mode of CytC interaction with the amyloid nanosurface might also play an important role. Since both CytC (isoelectric point (pI) = 10.5) and the amyloid nanosurface are cationic, it is most probable that hydrophobic interactions dominate this binding.[10] Notably, hydrophobic peptide segments of CytC from residues 81–85 have previously been reported to interact with hydrophobic surfaces.[10] This hydrophobic patch might be responsible for binding to the amphiphilic amyloid nanosurface, which also offers hydrophobic binding pockets.[5a] Interestingly, the nature of this binding might cause the heme crevice, which features a ring of lysine residues (positions 8, 13, 27, and 79),[11] to face away from the cationic nanosurface and thus

show better accessibility to substrates.[10,11] Finally, bound CytC was stable for up to 3 days at pH 7 (see Figures S7, S8 for a study in which the pH values were varied).

This study therefore shows the development of a unique class of remarkably active and soluble amyloid–protein nanohybrids in organic solvents. These nanohybrids could have potential practical applications given the small amount of amyloid nanostructures required. Furthermore, the simplicity of the preparation of these protein–amyloid hybrids, coupled with the design flexibility of the peptide hosts, make the present method adaptable for industrial applications.

Keywords: amyloids · cytochrome C · enzyme activity · immobilization · peroxidase

How to cite: *Angew. Chem. Int. Ed.* **2015**, *54*, 6492–6495
Angew. Chem. **2015**, *127*, 6592–6595

[1] a) J. D. Sipe, A. S. Cohen, *J. Struct. Biol.* **2000**, *130*, 88–98; b) I. W. Hamley, *Chem. Rev.* **2012**, *112*, 5147–5192.

[2] a) A. K. Mehta, K. Lu, W. S. Childers, Y. Liang, S. N. Dublin, J. Dong, J. P. Snyder, S. V. Pingali, P. Thiyagarajan, D. G. Lynn, *J. Am. Chem. Soc.* **2008**, *130*, 9829–9835; b) A. Laganowsky, C. Liu, M. R. Sawaya, J. P. Whitelegge, J. Park, M. Zhao, A. Pensalfini, A. B. Soriaga, M. Landau, P. K. Teng, D. Cascio, C. Glabe, D. Eisenberg, *Science* **2012**, *335*, 1228–1231; c) J. P. Colletier, A. Laganowsky, M. Landau, M. Zhao, A. B. Soriaga, L. Goldschmidt, D. Flot, D. Cascio, M. R. Sawaya, D. Eisenberg, *Proc. Natl. Acad. Sci. USA* **2011**, *108*, 16938–16943; d) I. W. Hamley, *Angew. Chem. Int. Ed.* **2007**, *46*, 8128–8147; *Angew. Chem.* **2007**, *119*, 8274–8295; e) A. J. Baldwin, T. P. J. Knowles, G. G. Tartaglia, A. W. Fitzpatrick, G. L. Devlin, S. L. Shammas, C. A. Waudby, M. F. Mossuto, S. Meehan, S. L. Gras, J. Christodoulou, S. J. Anthony-Cahill, P. D. Barker, M. Vendruscolo, C. M. Dobson, *J. Am. Chem. Soc.* **2011**, *133*, 14160–14163; f) A. J. Baldwin, S. J. Anthony-Cahill, T. P. J. Knowles, G. Lippens, J. Christodoulou, P. D. Barker, C. M. Dobson, *Angew. Chem. Int. Ed.* **2008**, *47*, 3385–3387; *Angew. Chem.* **2008**, *120*, 3433–3435.

[3] a) D. Li, H. Furukawa, H. Deng, C. Liu, O. M. Yaghi, D. S. Eisenberg, *Proc. Natl. Acad. Sci. USA* **2014**, *111*, 191–196; b) J. Boekhoven, S. I. Stupp, *Adv. Mater.* **2014**, *26*, 1642–1659; c) C. Li, J. Adamcik, R. Mezzenga, *Nat. Nanotechnol.* **2012**, *7*, 421–427; d) N. Even, L. Adler-Abramovich, L. Buzhansky, H. Dodiuk, E. Gazit, *Small* **2011**, *7*, 1007–1011; e) C. J. Forman, A. A. Nickson, S. J. Anthony-Cahill, A. J. Baldwin, G. Kaggwa, U. Feber, K. Sheikh, S. P. Jarvis, P. D. Barker, *ACS Nano* **2012**, *6*, 1332–1346; f) A. J. Baldwin, R. Bader, J. Christodoulou, C. E. MacPhee, C. M. Dobson, P. D. Barker, *J. Am. Chem. Soc.* **2006**, *128*, 2162–2163.

[4] a) Y. Zhang, R. Zhou, J. Shi, N. Zhou, I. R. Epstein, B. Xu, *J. Phys. Chem. B* **2013**, *117*, 6566–6573; b) L. S. Birchall, S. Roy, V. Jayawarna, M. Hughes, E. Irvine, G. T. Okorogheye, N. Saudi, E. De Santis, T. Tuttle, A. A. Edwards, R. V. Ulijn, *Chem. Sci.* **2011**, *2*, 1349–1355; c) D. Wu, J. Zhou, J. Shi, X. Du, B. Xu, *Chem. Commun.* **2014**, *50*, 1992–1994; d) P. A. Korevaar, C. J. Newcomb, E. W. Meijer, S. I. Stupp, *J. Am. Chem. Soc.* **2014**, *136*, 8540–8543; e) C. Ren, J. Zhang, M. Chen, Z. Yang, *Chem. Soc. Rev.* **2014**, *43*, 7257–7266; f) J. Wang, X. Miao, Q. Fengzhao, C. Ren, Z. Yang, L. Wang, *RSC Adv.* **2013**, *3*, 16739–16746; g) P. W. J. M. Frederix, G. G. Scott, Y. M. Abul-Haija, D. Kalafatovic, C. G. Pappas, N. Javid, N. T. Hunt, R. V. Ulijn, T. Tuttle, *Nat. Chem.* **2015**, *7*, 30–37; h) S. K. M. Nalluri, C. Berdugo, N. Javid, P. W. J. M. Frederix, R. V. Ulijn, *Angew. Chem. Int. Ed.* **2014**, *53*, 5882–5887; *Angew. Chem.* **2014**, *126*, 5992–5997; i) M. Reches, E. Gazit, *Nano Lett.* **2004**, *4*, 581–585; j) M. Reches, E. Gazit, *Science* **2003**, *300*, 625–627; k) Y. Gao, F. Zhao, Q. Wang, Y. Zhang, B. Xu, *Chem. Soc. Rev.* **2010**, *39*, 3425–3433; l) Q. Wang, Z. Yang, L. Wang, M. Ma, B. Xu, *Chem. Commun.* **2007**, 1032–1034; m) Q. Wang, Z. Yang, X. Zhang, X. Xia, C. K. Chang, B. Xu, *Angew. Chem. Int. Ed.* **2007**, *46*, 4285–4289; *Angew. Chem.* **2007**, *119*, 4363–4367; n) Q. Wang, Z. Yang, Y. Gao, W. Ge, L. Wang, B. Xu, *Soft Matter* **2008**, *4*, 550–553.

[5] a) W. S. Childers, A. K. Mehta, K. Lu, D. G. Lynn, *J. Am. Chem. Soc.* **2009**, *131*, 10165–10172; b) S. Li, A. N. Sidorov, A. K. Mehta, A. J. Bisignano, D. Das, W. S. Childers, E. Schuler, Z. Jiang, T. M. Orlando, K. Berland, D. G. Lynn, *Biochemistry* **2014**, *53*, 4225–4227; c) W. S. Childers, A. K. Mehta, R. Ni, J. V. Taylor, D. G. Lynn, *Angew. Chem. Int. Ed.* **2010**, *49*, 4104–4107; *Angew. Chem.* **2010**, *122*, 4198–4201.

[6] a) T. Kar, S. K. Mandal, P. K. Das, *Chem. Commun.* **2012**, *48*, 8389–8391; b) R. E. M. Diederix, M. Ubbink, G. W. Canters, *Eur. J. Biochem.* **2001**, *268*, 4207–4216.

[7] a) A. M. Klibanov, *Nature* **2001**, *409*, 241–246; b) N. Bruns, J. C. Tiller, *Nano Lett.* **2004**, *5*, 45–48; c) N. Bruns, W. Bannwarth, J. C. Tiller, *Biotechnol. Bioeng.* **2008**, *101*, 19–26; d) S. Konieczny, M. Leurs, J. C. Tiller, *ChemBioChem* **2015**, *16*, 83–90; e) X. Qian, A. Levenstein, J. E. Gagner, J. S. Dordick, R. W. Siegel, *Langmuir* **2014**, *30*, 1295–1303; f) A. L. Serdakowski, J. S. Dordick, *Trends Biotechnol.* **2008**, *26*, 48–54; g) D. Das, P. K. Das, *Langmuir* **2009**, *25*, 4421–4428; h) L. Dai, A. M. Klibanov, *Proc. Natl. Acad. Sci. USA* **1999**, *96*, 9475–9478; i) J. L. Schmitke, C. R. Wescott, A. M. Klibanov, *J. Am. Chem. Soc.* **1996**, *118*, 3360–3365; j) S. Maiti, M. Ghosh, P. K. Das, *Chem. Commun.* **2011**, *47*, 9864–9866; k) A. Grotzky, E. Altamura, J. Adamcik, P. Carrara, P. Stano, F. Mavelli, T. Nauser, R. Mezzenga, A. D. Schlüter, P. Walde, *Langmuir* **2013**, *29*, 10831–10840.

[8] K. Lu, L. Guo, A. K. Mehta, W. S. Childers, S. N. Dublin, S. Skanthakumar, V. P. Conticello, P. Thiyagarajan, R. P. Apkarian, D. G. Lynn, *Chem. Commun.* **2007**, 2729–2731.

[9] J. Kyte, R. F. Doolittle, *J. Mol. Biol.* **1982**, *157*, 105–132.

[10] a) L. Rivas, D. H. Murgida, P. Hildebrandt, *J. Phys. Chem. B* **2002**, *106*, 4823–4830; b) S. H. Speck, S. F. Miller, N. Osheroff, E. Margoliash, *Proc. Natl. Acad. Sci. USA* **1979**, *76*, 155–159.

[11] a) H. T. Smith, N. Staudenmayer, F. Millett, *Biochemistry* **1977**, *16*, 971–4974; b) R. Rider, H. R. Bosshard, *J. Biol. Chem.* **1980**, *255*, 4732–4739.

Received: February 2, 2015
Revised: March 3, 2015
Published online: April 7, 2015

